 https://doi.org/10.3311/PPci.22666

Periodica Polytechnica Civil Engineering, 69(1), pp. 210–219, 2025

Performance Evaluation of Wet Paving Concrete Incorporating Ternary Blends of Alluvial Tuff and Limestone Aggregates Using Simplex Centroid Mixture Method

Kianoush Siamardi[1], Masume Afshar[1], Shahin Shabani[2*]

[1] Department of Research and Development, Aptus Iran Company, St.113 Eram Blvd., Mehrshahr, 318694885 Karaj, Iran
[2] Department of Civil Engineering, Payame Noor University (PNU), P. O. B. 19395-4697, 19569 Tehran, Iran
* Corresponding author, e-mail: Shabani@pnu.ac.ir

Received: 26 May 2023, Accepted: 15 October 2024, Published online: 24 October 2024

Abstract

Incorporating the blends of aggregates from local quarries is inevitable for sustainable construction of concrete structures. In the present study, the performance of wet paving concrete (WPC) made with ternary blends of alluvial tuff (AF.Agg) and crushed limestone aggregates (LSLQ and LSHQ) were investigated using the simplex centroid mixture method (SCMM). The performance of WPC including the compressive strength (f_c), fracture energy (G_C) in compression, durability factor (D_f) after 300 freeze-thaw (FT) cycles in water, and the coefficient of thermal expansion (CTE) were measured according to the standard test procedures. A novel procedure was developed to measure the weight loss (W_L) and water absorption (W_A) of sawn cut prisms (SCPs) under the harsh exposure condition including 50 continuous salt-FT cycles with the high temperature gradient (−24 to +24 °C). The procedure was more destructive after a shorter exposure time. Non-linear correlations established between G_C & W_A with W_L indicating the pivotal role of interfacial bond in the long-term durability of WPC. The direct relation between W_L and W_A confirmed the porosity evolution of concrete matrix under the harsh exposure. The meaningful correlations were found between CTE and the other responses implying that an increase in CTE due to the presence of altered siliceous-based minerals within the aggregates have led to the weak interfacial bond of aggregate-paste under mechanical loads and eventually the earlier pop-out of particles under the harsh exposure. The empirical models were developed with the significant predictability to estimate the optimal blending ratio without compromising the concrete performance.

Keywords

wet paving concrete (WPC), ternary blending ratio, freeze-thaw durability, water absorption, fracture energy, harsh exposure condition

1 Introduction

Concrete mixes for paving blocks are proportioned to hold edges after passing through the vibrating paver. In hardened state, concrete should be strong and durable enough to withstand both traffic loads and freeze-thaw (FT) cycles in the presence of deicing salts [1]. Under this coupling action, continuous nucleation, formation and propagation of micro-cracks through the weakest link of concrete matrix like interfacial transition zone (ITZ) at the aggregate-paste interface increase the porosity and width of the ITZ. Eventually, this process makes concrete prone to other deteriorative reactions [2, 3]. Hence, the long-term serviceability of the plain concrete is still controversial issue [4]. Among practices enhancing the salt FT durability of concrete, addition of air-entraining agents (AEAs) to maintain 6% entrained air (Vol.) within the paste was more cost-effective in mitigating deformations as residual strain generated under accumulated and irreversible deterioration process [5–7]. Accordingly, as the FT durability in water (D_f) decreased to 60, the water absorption (W_A) increased from 3% to 6% indicating the more generated pores through the concrete after deterioration [3, 8]. Among the mix variables, aggregate characteristics especially coarse sizes play a pivotal role in the concrete performance [9, 10]. During the cement hydration, chemical reaction between $CaCO_3$ crystals in limestone and cement phases yields carbo-aluminate phases with more regular $Ca(OH)_2$ crystals leading to the better quality of ITZ followed by less coefficient of thermal expansion (CTE) along a thinner width of the ITZ compared to natural gravels that predominately composed of siliceous minerals [11]. A recent study revealed that the micro-hardness of ITZ for concretes made with limestone aggregates (LS.Agg)

Cite this article as: Siamardi, K., Afshar, M., Shabani, S. "Performance Evaluation of Wet Paving Concrete Incorporating Ternary Blends of Alluvial Tuff and Limestone Aggregates Using Simplex Centroid Mixture Method", Periodica Polytechnica Civil Engineering, 69(1), pp. 210–219, 2025. https://doi.org/10.3311/PPci.22666

was greater compared to those with natural aggregates (N.Agg) [12]. Gu et al. [13] found that the bond strength of ITZ was about half of the matrix strength. Besides, Nakamura et al. [14] necessitated investigating the effect of aggregates type and size on the concrete fracture under compressive failure (G_C) to further identify the characteristics of ITZ. Wu et al. [15] also stated that the G_C is a function of the concrete compressive strength (f_c) where the fracture takes place through the coarse aggregates. Generally, diversity in the mechanical, durability and thermal behavior of concrete were generally attributed to the morphology, texture, mineralogy, microstructure and stiffness of aggregates [16–19]. For concrete made with N.Agg, CTE was more than two times of that with LS.Agg while the higher CTE could aggravate the thermal stress caused by FT cycles in salt solution and eventually leads to the thicker ITZ [16, 20]. Cai et al. [21] also pointed out that excessive portion of coarse gravels can absorb more water during the FT cycles, and thereby increase the penetration depth of chloride salt solution.

To improve the most specifications regarding workability, mechanical and durability properties of concrete, blending of aggregates from local sources is recommended to attain the sustainable construction [22]. Tiegoum Wembe et al. [23] concluded that it's suitable to use up to 65% of crushed sand as partial replacement of river sand for concretes with water-to-cement ratio (*w*/*c*) ranged from 0.35 to 0.45. Médici et al. [24] have found a non-monotonic correlation between strength and portion of crushed aggregates blended with N.Agg due to variety in the aggregates properties. Koubaa et al. [25] recommended the incorporation of less-durable aggregates lower than 20% into concrete to give dilation <0.025% and D_f > 90. Some studies have concluded that the use of rough and angular crushed aggregates in high strength concrete could not definitely meet both the mechanical and durability specifications [26, 27]. The lower strength and higher permeability of concretes made with limestone and tuff aggregates compared to those with granite and andesite [28]. Even though each aggregate has its certain mineral composition and formation process, it's difficult to generalize these characteristics to the properties of concrete [29]. Therefore, employing the numerical simulation is required to simplify the prediction of concrete behavior according to the properties of aggregates [23]. In this regard, the design of experiment (DOE)- mixture approach has been confirmed as a robust tool to find optimal blends of aggregates with different characteristics for the production of sustainable concrete structures [30]. Accordingly, Adiguzel et al. [31] determined the optimal blend of aggregates from three quarries to mitigate the potential of alkali-silica reactivity of concrete. Siamardi et al. [32] optimized the blends of coarse and fine crushed LS.Agg from two local sources to produce sustainable paving concretes.

2 Objectives and research significance

The research objective is to investigate the hardened performance of wet paving concrete (WPC) incorporating ternary blends of alluvial tuff aggregates (AF.Agg) and two types of crushed LS.Agg from three local quarries. In short, f_c, stress-strain (σ–ε) curves and G_C as the mechanical responses, CTE as the thermal behavior, and WL, W_A, D_f as the durability parameters were measured and recorded as the concrete performance. To explore the influence of the aggregates on the concrete performance, different blending ratios were proportioned according to the DOE-simplex centroid mixture whilst the volume and properties of cement paste were fixed. The performance of the WPC in terms of blending ratios of aggregates was then correlated using the DOE-simplex centroid mixture method (SCMM) to establish regression models and thereby ascertain optimal blends. The interaction of these performance responses is analyzed for the first time to reveal the effect of blended aggregates on the properties of WPC. Finally, to fulfill the sustainable use of concrete aggregates, deteriorated concrete specimen made with an optimal blend after exposure to the harsh condition of salt-freezing and thawing is also explored via the scanning electron microscopy (SEM).

3 Experimental methods

3.1 Materials

A type II Portland cement from Tehran plant was used as binder in which the 28-days compressive strength of standard mortar and the Blaine fineness were 34 MPa and 3080 cm^2/g, respectively. A type-G poly-carboxylate ether-based superplasticizer (PCE) and ASTM C260-10 [33] were used as the chemical additives. The three types of aggregates from local mines including the AF.Agg, low (LSLQ) and high (LSHQ) quality crushed limestone aggregates with the properties given in Table 1 were incorporated.

As previously recommended [32, 34], the state of cementation and pore structure within the aggregates were well distinguished by the wet attrition of micro-deval and the FT test in a confined exposure, respectively.

Table 1 Properties of the coarse and fine aggregates used for manufacturing the WPC

Properties	Coarse			Fine		
	AF.Agg	LSLQ	LSHQ	AF.Agg	LSLQ	LSHQ
Rodded unit weight (kg/m^3)	1450	1490	1570	1630	1710	1660
Water absorption (%)	1.8	0.6	0.4	2.9	2	1.3
Specific gravity	2.58	2.69	2.7	2.6	2.71	2.72
Particles finer than 75 µm (%)	0.6	0.9	0.6	2.9	5.4	4.7
Potential alkali reactivity in 14 days (%)	-	-	-	0.076	0.028	0.011
Magnesium sulfate soundness (MSS) (%)	1.6	1.5	0.45	6.4	4.3	3.5
Freezing & thawing (%)	8.8	12.9	6.3	5.4	9	6.1
Los Angeles abrasion resistance (%)	14	26	25	18	24	23
Abrasion in micro-deval (%)	13.6	17.2	10.8	-	-	-
Flakiness / Elongation index (%)	17/22	16/28	10/24	-	-	-
Aggregate crushing value (ACV) (%)	15.7	22.3	20.1	-	-	-

Also, thin-section photomicrographs of aggregates under crossed polarized light (XPL) are shown in Fig. 1. The analysis revealed that LSHQ particles composed mainly of well-sorted matrix of clay-size calcium carbonate (micrite) whereas the AF.Agg composed of volcanic glass matrix and LSLQ had a poorly sorted micrite matrix in which both the AF.Agg and LSLQ contained altered minerals (i.e. strained quartz, rock fragments, iron-hydroxide) with micro-fissures leading to the more expansion of mortar in sodium-hydroxide solution as per ASTM C1260-14 [35, 36].

Fig. 1 XPL thin-section photomicrographs of aggregates

3.2 Mix design

The concrete mixes were design as per ACI PRC-211.1-91 [37] to give f_c = 40 MPa, 6% air content and 5 cm slump. The content of cement 415 kg, water 145 kg, PCE 2 kg, AEA 0.28 kg per one cube of concrete were fixed where 10 ternary blending ratios of aggregates as proportioned using the DOE-SCMM were incorporated. The gradation curves of coarse and fine aggregates with the combined gradations close to the power 0.45 curve are exhibited in Fig. 2. To ensure that a perfect bond at the aggregate-paste interface is accommodated, the *w/c* of 0.35 was considered to compensate the adverse effect of entrained air voids within the paste on the concrete strength.

3.3 Test methods

All the hardened tests were carried out after laboratory curing at the age of 28 days and the average of each set of experiments was considered as the performance response.

The 150 mm cubes were used for measuring f_c as per UNI EN 12390-3:2003 [38] where σ–ε curve of each mix

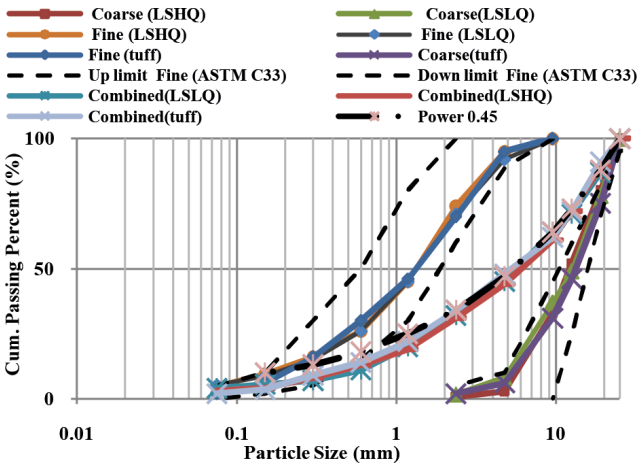

Fig. 2 Particle size distributions of aggregates

was recorded and the area under each curve was calculated to quantify the G_C of concrete. The CTE (strain variation affected by temperature gradient 10–50 °C) of cylinders (D100 × H200 mm^2) was measured as per AASHTO TP 60-00 (2007) [39]. The D_f of prisms (75 × 100 × 400 mm^3) in terms of the relative dynamic modulus of elasticity (RDME) after 300 FT cycles in water as per ASTM C666/C666M-15 [40] was also measured. As the harsh exposure condition, a procedure was developed to deteriorate the sawn prisms (75 × 100 × 30 mm^3) within 50 salt-FT cycles (−24 °C/16 h, +24 °C/8 h) to estimate the weight loss (W_L) [32]. The water absorption (W_A) of the deteriorated sawn cut prisms (SCPs) was measured after immersion in +40 °C water for 48 h.

4 Results and discussion

A total of 6 responses of the WPC affected by 10 ternary blending ratios of aggregates are given in Table 2. The σ–ε curves of WPC are shown in Fig. 3. As exhibited in Fig. 4, W_L increased dramatically after fewer number of salt-FT cycles compared to the decline in RDME as shown in Fig. 5. It could be attributed to the smaller size of SCPs which had been pre-stressed due to the cutting process before initiating the harsh exposure condition.

In addition, the SCPs were found more vulnerable under the harsh exposure due to their higher degree of saturation than those standard prisms [32, 41, 42]. The images of fragmented aggregate particles after 50 FT cycles confined in water as per AASHTO T 103 [43], deteriorated SCPs after the severe (harsh) exposure and the broken cubes under compression are shown in Fig. 6.

Furthermore, the strong correlations of G_C and W_A with W_L are depicted in Fig. 7 implying that a rise in G_C due to the better interfacial bond as well as the coarse aggregate characteristics could give durable and strong mixes under the harsh exposure as developed in the present research. This finding is partially consistent with some conclusions such that natural coarse aggregates composed of clastic particles, porous structure and smooth surface were more susceptible to pop-out and disintegration [3, 14, 18, 34].

As shown in Fig. 8 (a), the post-damage W_A increased dramatically rather than pre-damage W_A with aggravation in deterioration of SCPs due to the formation of new pores, nucleation, micro-cracks, and the propagation of pre-existing cracks particularly at the ITZ as concluded by [3, 42] that led to the more pop-out of coarse aggregates and loosely bonded particles from the matrix. Moreover, as confirmed by Yang et al. [8], W_A increased definitely with decline in G_C of concretes due to the irregular pore structure and micro-cracks through the matrix which were then exacerbated by the formation of inter-connected pores under the harsh exposure condition.

4.1 Development of simplex centroid mixture model

The DOE-SCMM was employed for equally weighted blending ratios of aggregates. The design consists of one centroid point (Mix No.6) and three secondary central points (Mix No.4,7,9) [44]. Accordingly, the responses of WPC were correlated with the blending ratios as the mix variables to establish the empirical models within the space and materials properties. The statistical evaluation of mixture model (Fig. 8 (b)) showed the lower error for 80% of fraction of design space (FDS). The fit summary and the analysis of variance (ANOVA) in the model are given in Table 3. Adequate precision as signal-to-noise ratio > 4 and (Adjusted R^2-Predicted R^2) < 0.2 indicate that the models could reliably be predictable. The overall variance inflation factor (VIF) of the model was less than 2 indicating an insignificant multi-collinearity.

Table 2 Results of experiments for each WPC mixture

Mix No.	Blending ratios of aggregates*			Performance responses					
	R_{Tuff}	R_{LSLQ}	R_{LSHQ}	f_c (MPa)	G_C (KJ/m^2)	CTE (με/°C)	W_L (%)	W_A (%)	D_f
1	1	0	0	37.7	6.8	8.7	6.12	4.89	67
2	0	0	1	53.4	13.7	4.5	0.78	0.95	89
3	0	0.5	0.5	48.7	11.4	5.6	2.14	2.62	82
4	0.666	0.167	0.167	42.9	8.6	7.5	4.06	4.45	70
5	0	1	0	43.4	9.8	5.8	3.1	3.34	72
6	0.333	0.333	0.333	47.8	10.1	6.2	2.73	3.47	76
7	0.167	0.666	0.167	46.3	10.3	6.6	2.64	3.67	75
8	0.5	0	0.5	47.6	9.7	5.9	2.8	3.11	74
9	0.167	0.167	0.666	51.5	11.9	5.2	1.37	2.14	82
10	0.5	0.5	0	42.8	8.8	7.4	3.86	4.32	69

* $R_{Tuff} + R_{LSLQ} + R_{LSHQ} = 1$

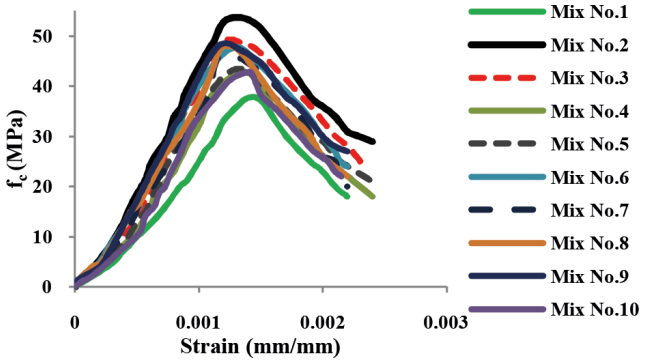

Fig. 3 Stress-strain curves of cubes under compression

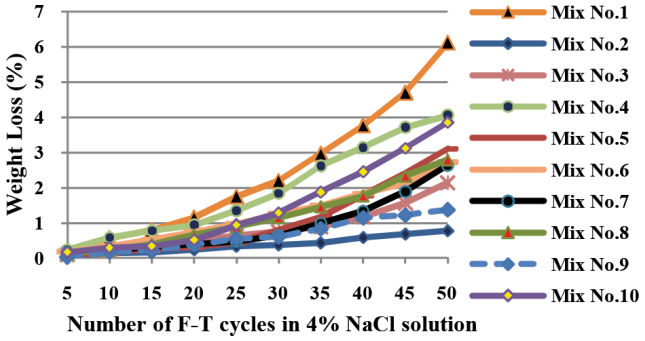

Fig. 4 W_L of SCPs per each 5 salt-FT cycles

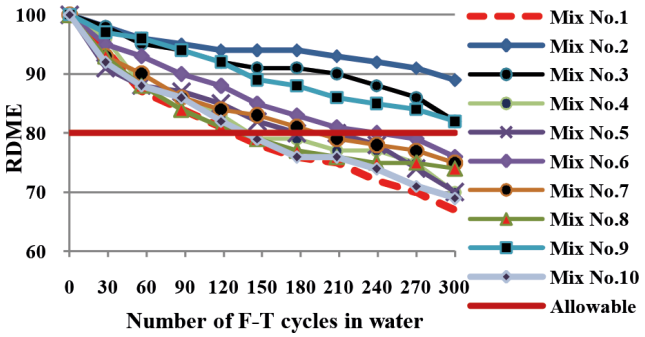

Fig. 5 RDME variations in standard prisms per each 30 FT cycles

Pearson's correlation factors relating the blending ratios to the studied responses are given in Table 3. As also approved from Fig. 8 (a), as the proportion of AF.Agg increased (e.g. Mix No.1), post-damage W_A was also increased significantly compared to the pre-damage W_A which could be attributed to the thicker ITZ, larger portlandite crystals, higher CTE and porous matrix. This results in the significant drop in G_C, f_c, D_f and increase in CTE, WL, W_A. These fluctuations could be attributed to the mineralogical characteristics of aggregates [11, 16, 21, 34].

4.2 Estimating the maximum aggregates incorporation

Using the prediction models, the maximum incorporation of aggregates was estimated to meet the specifications regarding the goals defined in Table 4. As the

Fig. 6 Images of fragmented particles of each quarry after FT cycles, SCPs after the harsh exposure and the broken cubes under compression

main goal, $D_f > 80$ was considered due to the fact that, a large number of pores contributes to the failure caused by frost action and a significant mechanical degradation could be anticipated for concretes with the lower D_f [45]. The other goals were set based on the statistical equivalency to meet the requirements, concurrently. Also, as confirmed by refs [11, 16, 20], Mix No.1 had the maximum CTE (8.7 με/°C) about 2 times of Mix No.2 due to the predominant altered siliceous minerals within porous structure of AF.Agg where the minimum G_C (6.8 KJ/m^2) about less than half of those with LSHQ aggregates was obtained due to the less interfacial bond. Thereby, these mixes were prone to sever degradation (W_L = 6.12%, D_f = 67, W_A = 3.24%→4.89%) under the harsh exposure.

Accordingly, further incorporation of AF.Agg (>13%) and LSLQ aggregates (>27%) with respect to the optimal blend may compromise the concrete performance. The contour plots for each response are shown in Fig. 9. The trend of contours for f_c, G_C, D_f and WL was similar whilst the trend for CTE and W_A followed the same pattern. The images of cross-section and SEM of the deteriorated SCP made with the optimal blend are shown in

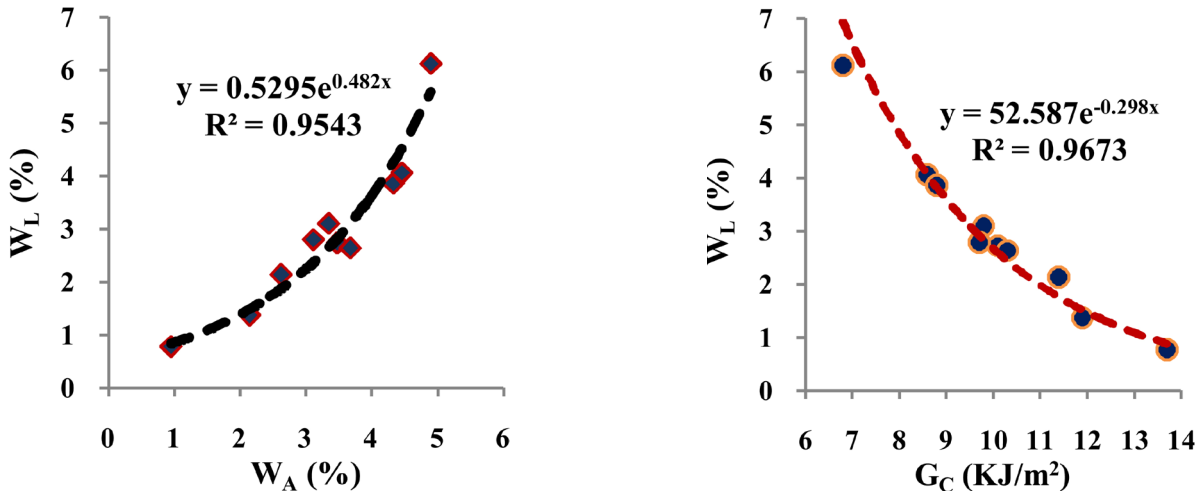

(a) (b)

Fig. 7 Non-linear correlations between (a) W_A and W_L, (b) G_C and W_L

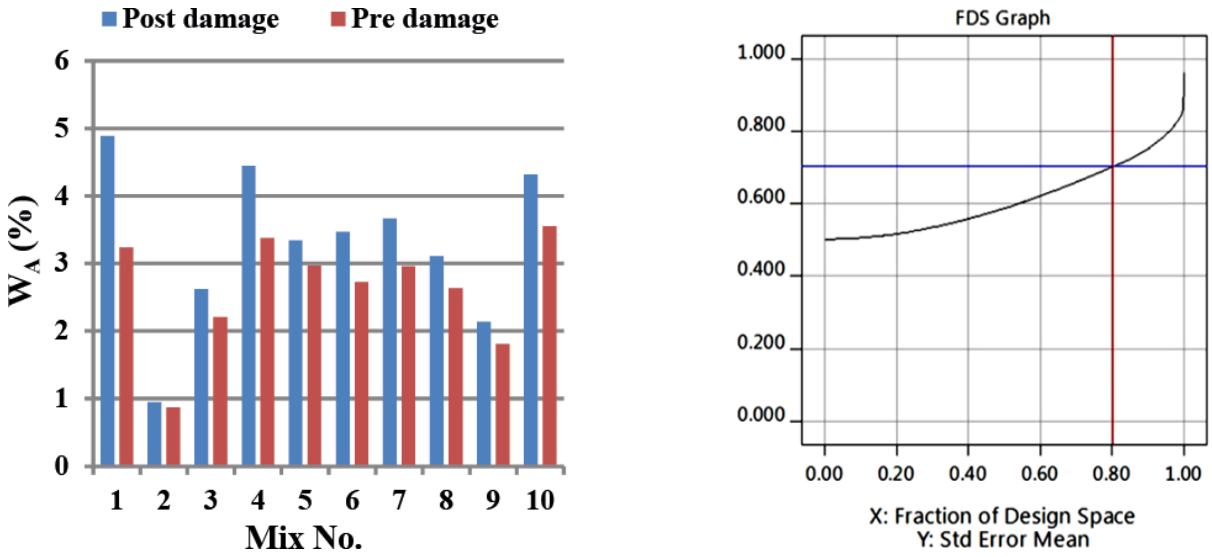

(a) (b)

Fig. 8 (a) Pre and post damage water absorption, (b) FDS graph vs. Standard error mean

Table 3 Fit summary and the ANOVA of the performance responses in the final model

Response	Pearson correlation factor			Fit statistics of the mixture models					
	R_{Tuff}	R_{LSLQ}	R_{LSHQ}	Regression	R^2	Adjusted R^2	Predicted R^2	Standard deviation	Adequate precision
f_c (MPa)	−0.741	−0.169	0.91	Quadratic	0.992	0.987	0.861	0.627	33.12
G_C (KJ/m²)	−0.844	−0.026	0.87	Quadratic	0.996	0.99	0.962	0.19	47
CTE (με/°C)	0.873	−0.067	−0.806	Quadratic	0.989	0.977	0.838	0.188	29.35
W_L (%)	0.862	−0.043	−0.819	Quadratic	0.993	0.984	0.919	0.18	37.23
W_A (%)	0.769	0.149	−0.918	Quadratic	0.992	0.983	0.853	0.15	34.8
D_f	−0.743	−0.186	0.928	Quadratic	0.997	0.992	0.957	0.6	47.5

Fig. 10. The weathering rind around the AF.Agg (green tuff) was observed indicating that these particles were susceptible to be detached from the matrix. Moreover, when the entrained air voids were critically saturated under the harsh exposure, cracks propagated through the pore fluid paths due to the formation of expansive products (e.g. calcium-oxychloride) [42] and excessive pressure caused by FT action where the bond at ITZ was weakened earlier.

Table 4 Estimation of maximum possible incorporation of aggregates

Variables and responses	Studied range	Goal	Theoretical prediction confidence 95%		
R_{Tuff}	0–1	predict	13	Prediction intervals (Low-High)	
R_{LSLQ}	0–1	predict	27		
R_{LSHQ}	0–1	predict	60		
f_c (MPa)	>49	In range	50.3	48.4	52.3
G_C (KJ/m^2)	>11	In range	11.6	11	12.2
CTE (με/°C)	<5.5	In range	5.5	4.9	6.1
W_L (%)	<2	In range	1.77	1.18	2.37
W_A (%)	<2.5	In range	2.5	2	3
D_f	>80	In range	81	80	83

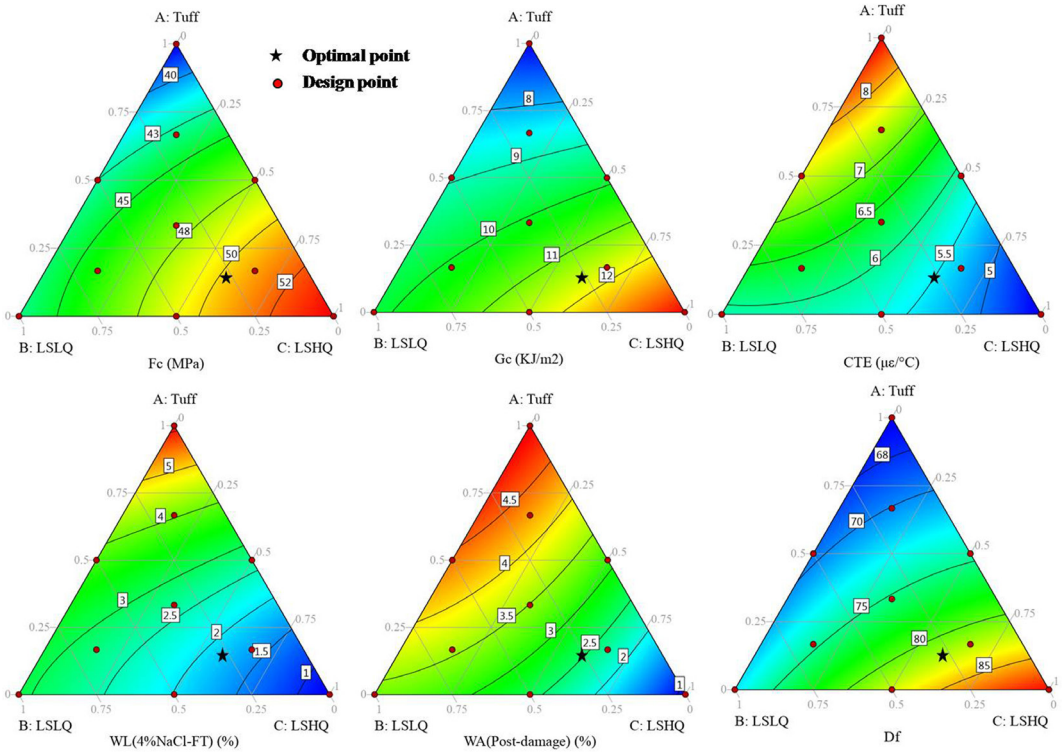

Fig. 9 Contour plots of responses generated by the mixture models in terms of ternary blending ratios with the optimal blend

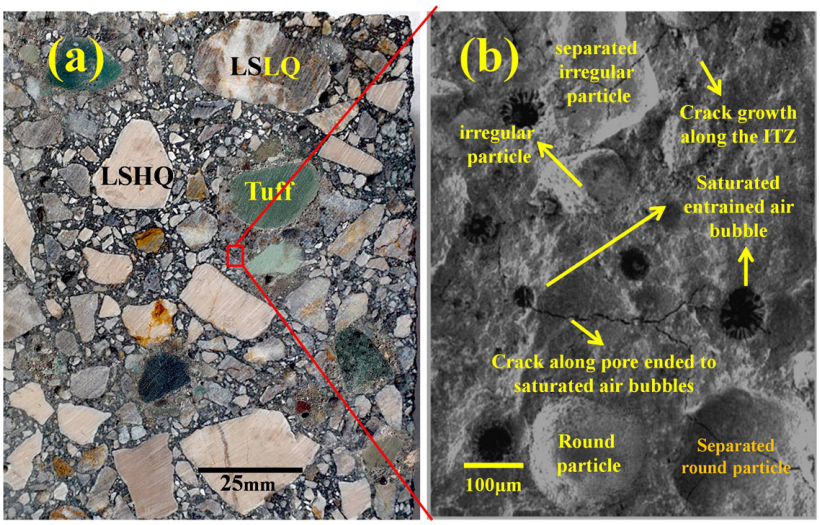

Fig. 10 Optimal SCP after harsh exposure: (a) Cross-section, (b) SEM

5 Conclusions

The thermal behaviour, mechanical properties and FT durability of the WPC made with different blending ratios of AF.Agg, LSLQ and LSHQ aggregates proportioned via DOE-SCMM were investigated while the volume and properties of air entrained paste were fixed. After then, the prediction models were developed to determine the maximum incorporation of aggregates without compromising the concrete performance. Consequently, the sawn prism made with the optimal blend subjected to the harsh exposure condition as a fast assessment and its micro-structure were studied. Based on the test results and analysis, the following conclusions were drawn:

1. The thin-section analysis of the aggregates was in conformity with the physical, mechanical and durability properties of aggregates as particularly evaluated through the micro-deval and FT tests.
2. Incorporation of AF.Agg into concrete mixes due to the higher CTE (8.7 με/°C) and the lower G_C (6.8 KJ/m^2) leading to the less strength and durability was limited to 13% to meet the specifications (f_c > 50 MPa & D_f > 80).
3. The SCPs under the harsh exposure condition underwent 50 FT cycles confined in 4% chloride salt solution with high temperature gradient (−24 to +24 °C) were more vulnerable especially for specimens made mainly with AF.Agg (W_L = 6.12%, W_A = 4.89%) than those standard prisms experienced FT cycles in water (D_f = 67).
4. Strong correlation was established between G_C and W_A with W_L which mainly dependent upon the mineralogy of aggregates, surface texture, and the ITZ. Accordingly, AF.Agg and LS.Agg were found to have adverse and positive effect on the WPC performance, respectively.
5. Difference in pre and post damage W_A of SCPs was significant for concretes made with extrusive AF.Agg due to the more porosity evolution under the harsh exposure condition whilst the negligible rise in W_A was pronounced for durable concretes made with crushed LSHQ aggregates having less CTE and perfect interfacial bond.
6. As a robust tool, the DOE-SCMM could generate predicting models to identify the concrete performance affected by different ratios of ternary blended aggregates.

Nomenclature

WPC = wet paving concrete
AF.Agg = alluvial tuff aggregate
R_{LSLQ} = ratio of low-quality limestone aggregates/total aggregates
R_{LSHQ} = ratio of high-quality limestone aggregates/total aggregates
R_{Tuff} = ratio of tuff aggregates/total aggregates
SCMM = simplex centroid mixture method
f_c = compressive strength of cubes at the age of 28-days
G_C = total fracture energy of cubes under compressive failure
D_f = durability factor after 300 freeze-thaw (FT) cycles in water
CTE = coefficient of thermal expansion of cylinders
W_L = weigh loss of sawn prisms after 50 FT cycles in salt solution
W_A = absorption of sawn prisms after 50 FT cycles in salt solution
SCP = sawn cut prism
ITZ = interfacial transition zone
LS.Agg = limestone aggregate
N.Agg = natural aggregate
DOE = design of experiment
PCE = poly-carboxylate ether-based superplasticizer
XPL = crossed polarized light
Micrite = clay size micro-crystalline calcium carbonate
RDME = relative dynamic modulus of elasticity
FDS = fraction of design space
ANOVA = analysis of variance
VIF = variance inflation factor

References

[1] Zapata, C. E., Andrei, D., Witczak, M. W., Houston, W. N. "Incorporation of environmental effects in pavement design", Road Materials and Pavement Design, 8(4), pp. 667–693, 2007. https://doi.org/10.1080/14680629.2007.9690094

[2] Craeye, B., Cockaerts, G., Kara De Maeijer, P. "Improving Freeze–Thaw Resistance of Concrete Road Infrastructure by Means of Superabsorbent Polymers", Infrastructures, 3(1), 4, 2018. https://doi.org/10.3390/infrastructures3010004

[3] Yang, X., Shen, A., Guo, Y., Zhou, S., He, T. "Deterioration mechanism of interface transition zone of concrete pavement under fatigue load and freeze-thaw coupling in cold climatic areas", Construction and Building Materials, 160, pp. 588–597, 2018. https://doi.org/10.1016/j.conbuildmat.2017.11.031

[4] Delatte, N. J. "Concrete Pavement Design, Construction, and Performance", [e-book] CRC Press, 2014. ISBN 9780429101786 https://doi.org/10.1201/b17043

[5] Zhao, H., Hu, Y., Tang, Z., Wang, K., Li, Y., Li, W. "Deterioration of concrete under coupled aggressive actions associated with load, temperature and chemical attacks: A comprehensive review", Construction and Building Materials, 322, 126466, 2022. https://doi.org/10.1016/j.conbuildmat.2022.126466

[6] Deja, J. "Freezing and de-icing resistance of blast furnace slag concrete", Cement and Concrete Composites, 25(3), pp. 357–361, 2003. https://doi.org/10.1016/S0958-9465(02)00052-5

[7] Du, P., Yao, Y., Wang, L., Xu, D., Zhou, Z., Sun, J., Cheng, X. "Using strain to evaluate influence of air content on frost resistance of concrete", Cold Regions Science and Technology, 157, pp. 21–29, 2019. https://doi.org/10.1016/j.coldregions.2018.09.012

[8] Yang, Z., Weiss, W. J., Olek, J. "Water Transport in Concrete Damaged by Tensile loading and Freeze-thaw Cycling", Journal of Materials in Civil Engineering, 18(3), pp. 424–434, 2006. https://doi.org/10.1061/(ASCE)0899-1561(2006)18:3(424)

[9] Hu, J., Wang, K. "Effects of coarse aggregate characteristics on concrete rheology", Construction and Building Materials, 25(3), pp. 1196–1204, 2011. https://doi.org/10.1016/j.conbuildmat.2010.09.035

[10] Yang, Y., Zhu, H., Chen, D. "Influence of the coarse aggregates size on the frost resistance in normal and polycarboxylate mixed concrete", Journal of Building Engineering, 76, 107031, 2023. https://doi.org/10.1016/j.jobe.2023.107031

[11] Teymen, A. "Statistical investigation of the effects of different origin aggregate properties on the mechanical properties of concrete", Revista de la Construcción. Journal of Construction, 22(2), pp. 482–508, 2023. https://doi.org/10.7764/RDLC.22.2.482

[12] Du, W., Qian, C. "Revealing the effect mechanism of calcareous aggregate and silica aggregate on the strength of ordinary concrete: Experiments, microscopic characterization, and molecular simulation", Journal of Building Engineering, 72, 106646, 2023. https://doi.org/10.1016/j.jobe.2023.106646

[13] Gu, X., Hong, L., Wang, Z., Lin, F. "Experimental study and application of mechanical properties for the interface between cobblestone aggregate and mortar in concrete", Construction and Building Materials, 46, pp. 156–166, 2013. https://doi.org/10.1016/j.conbuildmat.2013.04.028

[14] Nakamura, H., Nanri, T., Miuraa, T., Roy, S. "Experimental investigation of compressive strength and compressive fracture energy of longitudinally cracked concrete", Cement and Concrete Composites, 93, pp. 1–18, 2018. https://doi.org/10.1016/j.cemconcomp.2018.06.015

[15] Wu, K.-R., Chen, B., Yao, W., Zhang, D. "Effect of coarse aggregate type on mechanical properties of high-performance concrete", Cement and Concrete Research, 31(10), pp. 1421–1425, 2001. https://doi.org/10.1016/S0008-8846(01)00588-9

[16] An, J., Kim, S. S., Nam, B. H., Durham, S. A. "Effect of Aggregate Mineralogy and Concrete Microstructure on Thermal Expansion and Strength Properties of Concrete", Applied Sciences, 7(12), 1307, 2017. https://doi.org/10.3390/app7121307

[17] Aquino, C., Inoue, M., Miura, H., Mizuta, M., Okamoto, T. "The effects of limestone aggregate on concrete properties", Construction and Building Materials, 24(12), pp. 2363–2368, 2010. https://doi.org/10.1016/j.conbuildmat.2010.05.008

[18] Vishalakshi, K. P., Revathi, V., Sivamurthy Reddy, S. "Effect of type of coarse aggregate on the strength properties and fracture energy of normal and high strength concrete", Engineering Fracture Mechanics, 194, pp. 52–60, 2018. https://doi.org/10.1016/j.engfracmech.2018.02.029

[19] Beushausen, H., Dittmer, T. "The influence of aggregate type on the strength and elastic modulus of high strength concrete", Construction and Building Materials, 74, pp. 132–139, 2015. https://doi.org/10.1016/j.conbuildmat.2014.08.055

[20] Berenji Shokatabad, M., Sarkar, A. "Temperature curling and gradient of roller-compacted concrete composite pavements", Construction and Building Materials, 353, 129008, 2022. https://doi.org/10.1016/j.conbuildmat.2022.129008

[21] Cai, J., Wang, D., Xu, G., Tian, Q., Guo, S. "Influence of Coarse Aggregate Concentration on the Frost Resistance of Non-Air-Entrained Concrete", Journal of Engineering, 2022(1), 5146686, 2022. https://doi.org/10.1155/2022/5146686

[22] Telloli, C., Aprile, A., Marrocchino, E. "Petrographic and Physical-Mechanical Investigation of Natural Aggregates for Concrete Mixtures", Materials, 14(19), 5763, 2021. https://doi.org/10.3390/ma14195763

[23] Tiegon Wembe, J., Mambou Ngueyep, L. L., Elat Assoua Moukete, E., Eslami, J., Pliya, P., Ndjaka, J.-M. B., Noumowe, A. "Physical, mechanical properties and microstructure of concretes made with natural and crushed aggregates: Application in building construction", Cleaner Materials, 7, 100173, 2023. https://doi.org/10.1016/j.clema.2023.100173

[24] Médici, M. E., Benegas, O. A., Uñac, R. O., Vidales, A. M. "The effect of blending granular aggregates of different origin on the strength of concrete", Physica A: Statistical Mechanics and its Applications, 391(5), pp. 1934–1941, 2012. https://doi.org/10.1016/j.physa.2011.10.034

[25] Koubaa, A., Snyder, M. B., Janssen, D. J. "Development and evaluation of D-cracking mitigation techniques", In: Proceedings pro025: International RILEM Workshop on Frost Damage in Concrete, Mineapolis, MN, USA, 2002, pp. 265–288. ISBN 2912143314

[26] Güçlüer, K. "Investigation of the effects of aggregate textural properties on compressive strength (CS) and ultrasonic pulse velocity (UPV) of concrete", Journal of Building Engineering, 27, 100949, 2020. https://doi.org/10.1016/j.jobe.2019.100949

[27] Zhao, Y., Duan, Y., Zhu, L., Wang, Y., Jin, Z. "Characterization of coarse aggregate morphology and its effect on rheological and mechanical properties of fresh concrete", Construction and Building Materials, 286, 122940, 2021. https://doi.org/10.1016/j.conbuildmat.2021.122940

[28] Naderi, M., Kaboudan, A. "Experimental study of the effect of aggregate type on concrete strength and permeability", Journal of Building Engineering, 37, 101928, 2021. https://doi.org/10.1016/j.jobe.2020.101928

[29] Moulay-Ali, A., Abdeldjalil, M., Khelafi, H. "An experimental study on the optimal compositions of ordinary concrete based on corrected dune sand—Case of granular range of 25 mm", Case Studies in Construction Materials, 14, e00521, 2021. https://doi.org/10.1016/j.cscm.2021.e00521

[30] DeRousseau, M. A., Kasprzyk, J. R., Srubar III, W. V. "Computational design optimization of concrete mixtures: A review", Cement and Concrete Research, 109, pp. 42–53, 2018. https://doi.org/10.1016/j.cemconres.2018.04.007

[31] Adiguzel, D., Bascetin, A., Baray, S. A. "Determination of Optimal Aggregate Blending to Prevent Alkali-Silica Reaction Using the Mixture Design Method", Journal of Testing and Evaluation, 47(1), pp. 43–56, 2019. http://doi.org/10.1520/JTE20160441

[32] Siamardi, K., Shabani, S., Mansourian, A. "Optimization of concrete mixes using mixture approach for slip-formed concrete pavement incorporating blends of limestone aggregates", Construction and Building Materials, 397, 132377, 2023. https://doi.org/10.1016/j.conbuildmat.2023.132377

[33] ASTM International "ASTM C260-10 Standard Specification for Air-Entraining Admixtures for Concrete", ASTM International, West Conshohocken, PA, USA, 2010. https://doi.org/10.1520/C0260-10

[34] Beyene, M., Meininger, R., Munoz, J. F. "Mineralogic and petrographic evaluation of aggregate quality – effect on compressive strength of concrete pavement", International Journal of Pavement Engineering, 24(2), 2088756, 2023. https://doi.org/10.1080/10298436.2022.2088756

[35] ASTM International "ASTM C1260-14 Standard Test Method for Potential Alkali Reactivity of Aggregates (Mortar-Bar Method)", ASTM International, West Conshohocken, PA, USA, 2014. https://doi.org/10.1520/C1260-14

[36] Boggs Jr, S. "Petrology of sedimentary rocks", [e-book] Cambridge University Press, 2009. ISBN 9780511719332 https://doi.org/10.1017/CBO9780511626487

[37] ACI Committee 211 "ACI PRC-211.1-91: Standard practice for selecting proportions for normal, heavyweight and mass concrete", American Concrete Institute, Farmington Hills, MI, USA, 2002.

[38] UNITRAIN "UNI EN 12390-3:2003 Testing Hardened Concrete - Compressive Strength of Test Specimens", UNITRAIN, Milano, Italy, 2003.

[39] AASHTO "AASHTO TP 60-00 (2007) Standard Method of Test for Coefficient of Thermal Expansion of Hydraulic Cement Concrete", American Association of State Highway and Transportation Officials, Washington, DC, USA, 2007.

[40] ASTM International "ASTM C666/C666M-15 Standard Test Method for Resistance of Concrete to Rapid Freezing and Thawing", ASTM International, West Conshohocken, PA, USA, 2015.

[41] Martínez-Martínez, J., Arizzi, A., Benavente, D. "The Role of Calcite Dissolution and Halite Thermal Expansion as Secondary Salt Weathering Mechanisms of Calcite-Bearing Rocks in Marine Environments", Minerals, 11(8), 911, 2021. https://doi.org/10.3390/min11080911

[42] Wang, X., Zhang, J., Wang, X., Taylor, P., Wang, K., Sun, X. "Exploration of Mechanisms of Joint Deterioration in Concrete Pavements regarding Interfacial Transition Zone", Advances in Civil Engineering, 2018, 3295954, 2018. https://doi.org/10.1155/2018/3295954

[43] AASHTO "AASHTO T 103 Standard Method of Test for Soundness of Aggregates by Freezing and Thawing", American Association of State Highway and Transportation Officials, Washington, DC, USA, 2008.

[44] Cornell, J. A. "A Primer on Experiments with Mixtures", [e-book] John Wiley & Sons, 2011. ISBN 9780470643389

[45] Zhang, W., Pi, Y., Kong, W., Zhang, Y., Wu, P., Zeng, W., Yang, F. "Influence of damage degree on the degradation of concrete under freezing-thawing cycles", Construction and Building Materials, 260, 119903, 2020. https://doi.org/10.1016/j.conbuildmat.2020.119903